Intercalation of Decamolybdodicobaltate(III) Anion in Layered Double Hydroxides

Juan J. Bravo-Suárez,[†,§] Edgar A. Páez-Mozo,[‡] and S. Ted Oyama*[,§]

Escuela de Ingeniería Química and Escuela de Química, Centro de Investigaciones en Catálisis, Universidad Industrial de Santander, A.A. 678 Bucaramanga, Colombia, and Environmental Catalysis and Nanomaterials Laboratory, Department of Chemical Engineering, Virginia Polytechnic Institute and State University, Blacksburg, Virginia 24061-0211

Received September 13, 2003. Revised Manuscript Received December 12, 2003

Intercalation of decamolybdodicobaltate(III) anion ($[Co_2Mo_{10}]$) in a MgAl layered double hydroxide (LDH) was carried out by an anion exchange reaction using MgAl−OH LDHs (meixnerite) as precursors. The synthesis of pure and crystalline LDHs intercalated with $[Co_2Mo_{10}]$ required trade-offs between different reaction conditions for the $[Co_2Mo_{10}]$ anions and the LDH layers to be stable to hydrolysis reactions. In this work, these conditions for intercalation were achieved using meixnerite precursors of Al/(Mg + Al) molar ratios larger than 0.33, a reaction pH of about 4.7, and a nonaqueous medium (ethanol/water 40 vol %) at 353 K, with an exchange time of 1 h. The structure and composition of the intercalates were established by elemental analysis, powder X-ray diffraction, FTIR and Raman spectroscopies, thermal methods, rehydration experiments, SEM and TEM microscopies, and N_2 adsorption/desorption studies. Gallery heights of 0.74 and 0.97 nm were observed for the $[Co_2Mo_{10}]$ intercalated LDHs, corresponding to two different anion orientations in the interlayers. The interlayer $[Co_2Mo_{10}]$ is stable up to 523 K and the layer structure is stable up to 573 K, even though the morphology of the intercalated materials is retained up to 773 K.

Introduction

Layered double hydroxides (LDHs) constitute a very important class of ionic solids particularly useful for the synthesis of pillared layered materials. LDHs are generally represented by the formula $[M^{2+}_{1-x}M^{3+}_{x}(OH)_2]^{x+}(A^{n-}_{x/n})\cdot mH_2O$, where M^{2+} is a divalent cation and M^{3+} is a trivalent cation, x is the ratio $M^{3+}/(M^{2+} + M^{3+})$ and A^{n-} can be almost any intercalating anion.[1] In the past decade great attention has been paid to the intercalation of large polyoxometalate (POMs) anions in LDHs because of their numerous potential uses, such as shape-selective catalysts[2−4] and as novel protonic conductors in electrochemical applications.[5] Several methods have been developed for the intercalation of POMs in LDH materials which include methods based on anion exchange using different precursors (A = NO_3^-, OH^-, CO_3^{2-}, adipate, terephthalate, triethyleneglycolate, etc.),[2,6−10] as well as various methods based on LDH-syntheses such as LDH reconstruction,[11−14] coprecipitation,[15−16] and chimie douce.[17−18] These POM intercalation methods are shown schematically in Figure 1.

Typical bulky intercalated POMs found in the literature possess semispherical Keggin type structure ($[X^{n+}M_{12}O_{40}]^{(8-n)-}$), such as $[BVW_{11}O_{40}]^{7-}$, $[H_2W_{12}O_{40}]^{6-}$, $[SiW_{11}O_{39}]^{8-}$, $[PV_nW_{12-n}O_{40}]^{(n+3)-}$ (n = 0, 2, 3, 4), $[PZW_{11}O_{39}]^{5-}$ (Z = Co^{2+}, Ni^{2+}, Cu^{2+}, Zn^{2+}, Fe^{2+}), and $[SiZW_{11}O_{39}]^{6-}$ (Z = Mn^{2+}, Fe^{2+}, Co^{2+}, Ni^{2+}, Cu^{2+}, Zn^{2+}) among others;[3−4,6,8−10,12,14−15,19−20] and structures originated from the polymerization of Keggin fragments (i.e., Wells−Dawson and Finke structures) such as $[P_2W_{17}O_{61}]^{10-}$, $[Zn_4(AsW_9O_{34})_2]^{10-}$, $[WZn_3(ZnW_9O_{34})_2]^{12-}$, $[P_4W_{30}Zn_4O_{112}]^{16-}$, $[NaSb_9W_{21}O_{86}]^{18-}$, $[NaP_5W_{30}O_{110}]^{14-}$, $[Ln(XW_{11}O_{39})_2]^{n-}$ (Ln = La^{3+}, Ce^{3+}, Ce^{4+}; X = P^{5+}, Si^{4+},

* To whom correspondence should be addressed. E-mail: oyama@vt.edu.
† Escuela de Ingeniería Química, Universidad Industrial de Santander.
‡ Escuela de Química, Universidad Industrial de Santander.
§ Virginia Polytechnic Institute and State University.

(1) Allman, R. *Neues Jahrb. Mineral., Monatsh.* **1969**, *12*, 544.
(2) Kwon, T.; Tsigdinos, G. A.; Pinnavaia, T. J. *J. Am. Chem. Soc.* **1988**, *110*, 3653.
(3) Gardner, E.; Pinnavaia, T. J. *Appl. Catal., A* **1998**, *167*, 65.
(4) Tatsumi, T.; Yamamoto, K.; Tajima, H.; Tominaga, H. *Chem. Lett.* **1992**, *5*, 815.
(5) Keita, B.; Belhouari, A.; Nadjo, L. *J. Electroanal. Chem.* **1993**, *355*, 235.
(6) Kwon, T.; Pinnavaia, T. J. *J. Mol. Catal.* **1992**, *74*, 23.
(7) Drezdzon, M. A. *Inorg. Chem.* **1988**, *27*, 4628.
(8) Kwon, T.; Pinnavaia, T. J. *Chem. Mater.* **1989**, *1*, 381.
(9) Dimotakis, E. D.; Pinnavaia, T. J. *Inorg. Chem.* **1990**, *29*, 2393.
(10) Wang, J.; Tian, Y.; Wang, R. C.; Clearfield, A. *Chem. Mater.* **1992**, *4*, 1276.
(11) Chibwe, K.; Jones, W. *Chem. Mater.* **1989**, *1*, 489.
(12) Narita, E.; Kaviratna, P.; Pinnavaia, T. *J. Chem. Lett.* **1991**, 805.
(13) Kooli, F.; Rives, V.; Ulibarri, M. A. *Inorg. Chem.* **1995**, *34*, 5114.
(14) Xu, Z.; He, H. M.; Zhou, D. M.; Wen, L. S.; Jiang, D. Z.; Wu, Y. *Chin. Chem. Lett.* **1995**, *6*, 719.
(15) Narita, E.; Kaviratna, P. D.; Pinnavaia, T. J. *J. Chem. Soc., Chem. Commun.* **1993**, 60.
(16) Kooli, F.; Jones, W. *Inorg. Chem.* **1995**, *34*, 6237.
(17) Han, K. S.; Guerlou-Demourgues, L.; Delmas, C. *Solid State Ionics* **1996**, *84*, 227.
(18) Vaysse, C.; Guerlou-Demourgues, L.; Demourgues, A.; Lazartigues, F.; Fertier, D.; Delmas, C. *J. Mater. Chem.* **2002**, *12*, 1035.

10.1021/cm034853c CCC: $27.50
Published on Web 03/02/2004

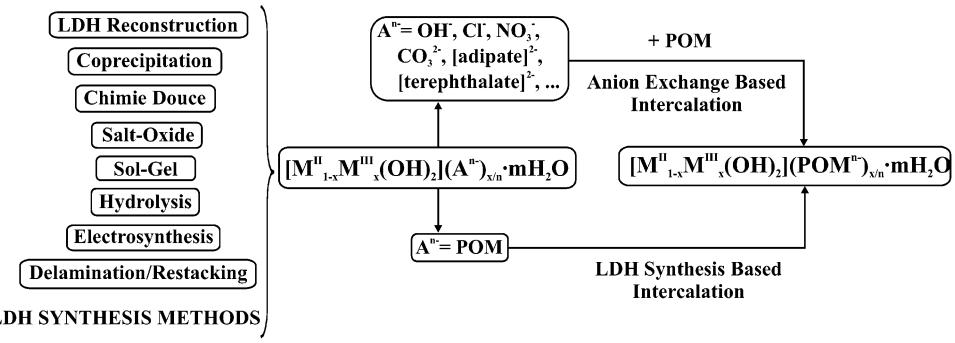

Figure 1. Intercalation methods of polyoxometalate anions in layered double hydroxides.

B^{3+}), etc.[19−23] Other oxometalates of medium-nuclearity include $[V_2O_7]^{4-}$, $[V_{10}O_{28}]^{6-}$, $[Mo_7O_{24}]^{6-}$, $[W_7O_{24}]^{6-}$, etc.[2,7,16−18,20,24−25]

The decamolybdodicobaltate(III) anion ($[H_4Co_2Mo_{10}O_{38}]^{6-}$, here denoted as $[Co_2Mo_{10}]$), is a POM that presents a distinctive structure which is perhaps the only one known of its kind.[26] The $[Co_2Mo_{10}]$ POM is formed by putting together two Andersen chiral fragments of $[CoMo_5]$. The enantiomers of $[Co_2Mo_{10}]$ present a D_2 symmetry and the racemic mixture as studied by Evans and Showell has the space group Pc.[27] Despite this uniqueness, the $[Co_2Mo_{10}]$ has been little studied and there is scant information in the literature concerning this POM. Recently, Cabello et al.[28] studied the $[Co_2Mo_{10}]$ anion as a possible precursor for the synthesis of Co−Mo/γ-Al_2O_3 hydrotreating catalysts. To the best of our knowledge, this has been the only publication regarding the application of the $[Co_2Mo_{10}]$ POM. In another paper, Zhao et al.[29] have reported the utilization of LDHs as precursors for the preparation of catalyst supports for the hydrodesulfurization of FCC gasoline. Additionally, very few molybdenum-containing POMs intercalated in LDHs have been reported, and among these the heptamolybdate intercalated LDH has presented remarkable results as a shape-selective catalyst in epoxidation reactions.[3,4] We have recently[30] estimated the textural properties of $Mg_{1-x}Al_x$-LDHs intercalated with $[Co_2Mo_{10}]$ POM by means of theoretical models. The obtained results suggested that microporous materials might be obtained for values of x lower than 0.25 (Mg/Al > 3.0). The fact that the $[Co_2Mo_{10}]$ POM is a chiral complex was of particular interest because its intercalation could produce a completely inorganic chiral microporous material. From these reports, we had expected that $[Co_2Mo_{10}]$ intercalated LDHs could be used as shape-selective catalysts in low and high-temperature applications. However, as will be shown, the material that resulted had low microporosity because of the dense packing of the POM pillars.

The purpose of the present work is to obtain a pure and crystalline LDH intercalated with $[Co_2Mo_{10}]$. Even though several methods of POM intercalation are available, the synthesis of this intercalate is not straightforward because the LDH layers are basic in nature and the $[Co_2Mo_{10}]$ anion is acidic, and the materials have different pH ranges of stability. The incompatibility in pH contributes to the partial hydrolysis of both the LDH layers and the POM anions. In this study successful synthesis of the intercalated compound was achieved by using a $Mg_{1-x}Al_x$−OH (for $x > 0.33$) LDH which was stable at a pH of 4.7 where the $[Co_2Mo_{10}]$ anion was still intact. Some factors studied in the intercalation process are the pH of the reaction medium, the temperature and the time of the exchange, and the influence of a nonaqueous medium (ethanol/water mixture) on the hydrolysis of the LDH layers and the $[Co_2Mo_{10}]$ anions. The characterization and physical properties of the new resulting materials are also reported.

Experimental Section

Materials. The following reagents were used as received without additional purification: $Mg(NO_3)_2{\cdot}6H_2O$ (Aldrich, ACS reagent), $Al(NO_3)_3{\cdot}9H_2O$ (Aldrich, ACS reagent), $Zn(NO_3)_2{\cdot}6H_2O$ (Aldrich, 98%), $Ni(NO_3)_2{\cdot}6H_2O$ (Alfa Aesar, technical grade), NaOH pellets (J. T. Baker, 98.7%), Na_2CO_3 anhydrous powder (J. T. Baker, ACS reagent), $NaNO_3$ (Fluka, ACS reagent), HNO_3 (VWR International, ACS reagent), compressed nitrogen (Airgas Inc., ultrapure carrier grade), tri(ethylene glycol) (Aldrich, 99%), ethanol (AAPER Alcohol and Chemical Co., 200 proof), $(CH_3CO_2)_2Co{\cdot}4H_2O$ (Aldrich, ACS reagent), $(NH_4)_6Mo_7O_{24}{\cdot}4H_2O$ (Aldrich, ACS reagent), H_2O_2 (EM Science, 30% aqueous solution), and activated carbon Darco KB (Aldrich, −100 mesh).

LDH Synthesis. The MgAl−CO_3 and MgAl−OH LDHs were prepared by methods similar to those described by Yun and Pinnavaia.[21] The MgAl−CO_3 LDHs were prepared by a coprecipitation method,[31] using a 3-L, three-necked flask equipped with two 250-ml burets, a thermocouple, a pH probe, a magnetic stirrer, and an electric heating mantle. The flask was charged with 400 mL of freshly distilled, deionized (DDI) water and the temperature was raised and controlled at 323 K. Drops of a 2 M NaOH solution were added to the vigorously stirred mixture until a pH of 10.0 was obtained. A 500-mL solution of 0.5 M metal nitrates of Mg^{2+} and Al^{3+} ($Al^{3+}/(Mg^{2+}+Al^{3+}) = 0.14$, 0.25, 0.33, and 0.40) was added dropwise

(19) Xu, L.; Hu, C. W.; Wang, E. B. *J. Nat. Gas Chem.* **1997**, *6*, 155.
(20) Rives, V.; Ulibarri, M. A. *Coord. Chem. Rev.* **1999**, *181*, 61.
(21) Yun, S. K.; Pinnavaia, T. J. *Inorg. Chem.* **1996**, *35*, 6853.
(22) Gardner, E. A.; Yun, S. K.; Kwon, T., Pinnavaia, T. J. *Appl. Clay. Sci.* **1998**, *13*, 479.
(23) Guo, Y.; Li, D.; Hu, C.; Wang, Y.; Wang, E. *Int. J. Inorg. Mater.* **2001**, *3*, 347.
(24) Twu, J.; Dutta, P. K. *J. Phys. Chem.* **1989**, *93*, 7863.
(25) Ulibarri, M. A.; Labajos, F. M.; Rives, V.; Trujillano, R.; Kagunya, W.; Jones, W. *Inorg. Chem.* **1994**, *33*, 2592.
(26) Pope, M. T. *Heteropoly and Isopoly Oxometalates*; Springer: Berlin, 1983.
(27) Evans, H. T., Jr.; Showell, J. S. *J. Am. Chem. Soc.* **1969**, *91*, 6881.
(28) Cabello, C. I.; Cabrerizo, F. M.; Alvarez, A.; Thomas, H. J. *J. Mol. Catal. A: Chem.* **2002**, *186*, 89.
(29) Zhao, R.; Yin, C.; Zhao, H.; Liu, C. *Fuel Process. Technol.* **2003**, *81*, 201.
(30) Bravo-Suárez, J. J.; Páez-Mozo, E. A.; Oyama, S. T. *Microporous Mesoporous Mater.* **2004**, *67*, 1.
(31) Cavani, F.; Trifiro, F.; Vaccari, A. *Catal. Today* **1991**, *11*, 173.

to the stirred aqueous solution via the buret over a time period of 80 min. Simultaneous addition of a mixed solution of 1 M Na_2CO_3 and 2 M NaOH ($CO_3^{2-}/Al^{3+} = 1.5$) was carried out manually to maintain a constant pH of 10.0 (± 0.2). Once the addition of the Na_2CO_3/NaOH solution was completed, the pH of the reaction was controlled by the addition of a 2 M NaOH solution. Following the complete addition of the mixed-metal salt solution, the white suspension was then aged at 343 K for 20 h. The white product was filtered, washed thoroughly with DDI water and dried overnight at 338 K. The MgAl−OH LDH slurries were prepared by the LDH reconstruction method.[32] First, 14 g of the MgAl−CO_3 LDH was placed in a quartz tube furnace, and the temperature was increased from room temperature to 773 K in 1 h, and kept at 773 K for 5 h under a N_2 flow. The obtained oxides were dispersed in DDI water (1.0 wt %) under N_2 and stirred at room temperature for 5 days, to form the MgAl−OH LDH (meixnerite).

Ammonium Decamolybdodicobaltate(III) Synthesis. Dark green crystals of ammonium decamolybdodicobaltate ($[NH_4]_6[H_4Co_2Mo_{10}O_{38}]\cdot 7H_2O$) are obtained from the reaction of ammonium heptamolybdate and cobalt acetate in the presence of hydrogen peroxide and activated carbon following the method of Tsigdinos.[33]

Intercalation of Decamolybdodicobaltate by Anion Exchange. A 0.015 M [Co_2Mo_{10}] POM solution in 3-fold excess of the anion exchange capacity was used for the intercalation procedure. The [Co_2Mo_{10}] POM was dissolved in either DDI water or an ethanol/DDI water mixture (40 vol %) depending on the reaction conditions. An aqueous slurry of MgAl−OH LDH was added dropwise over a time period of about 0.25 h to the [Co_2Mo_{10}] POM solution under N_2, and was stirred vigorously at the selected reaction temperature and pH. Selected pH values for the anion exchange were as follows: autogenous pH (resulting from the mixing of the LDH slurry and the POM solution), pH 4.7 (approximately the pH of a 0.015 M [Co_2Mo_{10}] solution in an ethanol/water 40 vol % mixture), and pH 4.3 (approximately the pH of a 0.015 M [Co_2Mo_{10}] solution in DDI water). When required, the pH was controlled by the addition of 1 M HNO_3 through all the time of the exchange. After exchange for a set time, the solids were separated by filtration and washed with hot DDI water (∼343 K) and dried overnight in air at room temperature.

Materials Characterization. Powder X-ray diffraction (PXRD) patterns were obtained with a Scintag XDS 2000 diffractometer using Cu Kα radiation at a scanning speed of 1.5° min^{-1}. Infrared spectra were recorded with a Digilab Excalibur FTS 3000MX spectrometer provided with a DTGS Peltier cooled detector; the resolution was 2 cm^{-1}, and 32 scans were averaged. Samples were prepared using the KBr pellet technique. Raman spectra were recorded on a system that used an argon ion laser (514.5 nm, Spex Lexel 95) as a light source, a holographic notch filter (Kaiser, Super Notch Plus) for removing Rayleigh scattering, a single stage monochromator (Spex, 500 M) for energy dispersion, and a CCD detector (Spex, Spectrum One) for spectral acquisition. The laser was operated at 50 mW and the detector slit width was set at 100 μm. The resolution of the Raman spectrometer was 6 cm^{-1}. Samples were ground and loaded into glass sampling tubes. N_2 adsorption experiments were performed at liquid-nitrogen temperature (77.3 K), using a Micromeritics ASAP 2000 apparatus (a static volumetric technique). Prior to the determination of an adsorption isotherm, samples (about 200 mg) were outgassed at different temperatures (378, 473, 573, 673, and 773 K) for 12 h. Surface areas were obtained by the BET method,[34] and the microporous areas and volumes were obtained by the t-plot method.[35] Thermogravimetric analyses were performed using a Seiko TG/DTA 220 thermal analyzer. The furnace was heated from room temperature to 773 K at a rate of 5 K min^{-1} in an air atmosphere. Scanning electron microscopy (SEM) images of the samples were taken on a LEO 1550 FESEM electron microscope at 5 kV. Electron micrographs were taken by the transmission electron microscopy method (TEM) at 100 kV with a Philips 420T TEM instrument. Samples for TEM were prepared by dipping a carbon-coated copper grid into an aqueous suspension of the solid and allowing the water to evaporate at room temperature. Chemical analyses for Mg, Al, Co, and Mo were carried out at the Virginia Tech Soil Testing Laboratory, using a Spectroflame FTMOA85D ICP-AES spectrometer made by Spectro Analytical Instruments. Samples were prepared by dissolving approximately 30 mg of solid in 50 mL of a 3 vol % HNO_3 solution. The pH values were measured with an OAKTON Acorn PH 6 meter fitted with a Cole-Palmer combination electrode.

Results and Discussion

The basic nature of the LDH layers and the acidic properties of the [Co_2Mo_{10}] anion make the intercalation process difficult. The following preliminary intercalation experiments using different methods were carried out. (a) Coprecipitation of aqueous $Ni(NO_3)_2$ and $Al(NO_3)_3$ ($Al/(Ni + Al) = 0.25$) with NaOH at pH 6 in the presence of [Co_2Mo_{10}] at room temperature, for 1 h, and drying at room temperature. (b) Anion exchange of a wet freshly prepared $Ni_{0.75}Al_{0.25}$−NO_3 LDH with [Co_2Mo_{10}] at pH 5.5 at room temperature, for 1 h, and drying at room temperature. (c) Anion exchange of a wet freshly prepared $Mg_{0.75}Al_{0.25}$−NO_3 LDH with [Co_2Mo_{10}] at 333 K, at autogenous pH, for 1.5 h, and drying at room temperature. (d) Anion exchange of a wet $Zn_{0.67}Al_{0.33}$−NO_3 LDH with [Co_2Mo_{10}] at room temperature, autogenous pH, for 6 h, and drying at room temperature. (e) LDH reconstruction of $Mg_{0.75}Al_{0.25}$-oxides ($Mg_{0.75}Al_{0.25}$−CO_3 calcined at 773 K for 5 h) slurried in a [Co_2Mo_{10}] solution at 373 K for 0.66 h and drying at room temperature. (f) Anion exchange of $Mg_{0.75}Al_{0.25}$-triethyleneglycolate (from $Mg_{0.75}Al_{0.25}$−CO_3 slurried in triethyleneglycol at 393 K for 5 h) and [Co_2Mo_{10}] solution at 353 K, autogenous pH, for 1 h, and drying at room temperature. (g) Anion exchange of $Mg_{0.75}Al_{0.25}$−OH (from $Mg_{0.75}Al_{0.25}$-oxides slurried in H_2O at room temperature for 5 days) and [Co_2Mo_{10}] solution at 358 K, autogenous pH, for 0.25 h, and drying at room temperature.

The X-ray powder diffraction patterns of the resulting materials are shown in Figure 2. As can be seen from Figure 2, crystalline intercalated materials giving sharp PXRD peaks can be prepared with the MgAl−OH LDH by the anion exchange method. The use of meixnerite LDHs (charge-compensating ion is OH^-) in the intercalation of Keggin-type POMs has been previously reported. For instance, Yun and Pinnavaia,[21] and Gardner et al.[22] have shown the usefulness of meixnerite compounds as precursors for the anion exchange of bulky POMs or as intermediates for the preparation of organo-anion precursors[9] later used in POM anion-exchange procedures. Thus, the anion exchange with meixnerite LDH compounds seems to be a general route for the intercalation of POMs. The use of freshly prepared LDH−OH materials is perhaps the key to the successful intercalation since the LDHs are fully hydrated and uncontaminated with carbonate anions, and this facilitates the anion exchange. Additional considerations in the anion exchange procedure include the

(32) Sato, T.; Kato, K.; Endo, T.; Shimada, M. *React. Solids* **1986**, *2*, 253.
(33) Tsigdinos, G. A. Ph.D. Thesis, Boston University, 1961.
(34) Brunauer, S.; Emmett, P. H.; Teller, E. *J. Am. Chem. Soc.* **1938**, *60*, 309.
(35) De Boer, J. H.; Linsen, B. G.; Osinga, T. H. J. *J. Catal.* **1965**, *4*, 643.

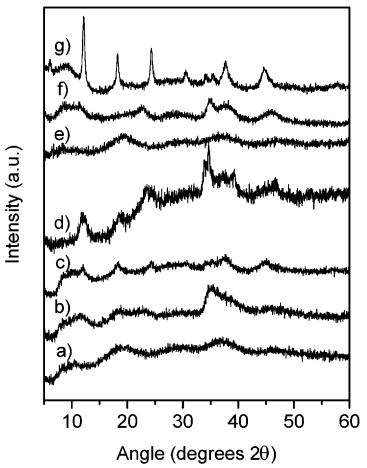

Figure 2. X-ray powder diffraction patterns of $[Co_2Mo_{10}]$ intercalated LDHs using different methods: (a) $Ni_{0.75}Al_{0.25}-Co_2Mo_{10}$ by coprecipitation; (b) $Ni_{0.75}Al_{0.25}-Co_2Mo_{10}$ by anion exchange ($Ni_{0.75}Al_{0.25}-NO_3$ precursor); (c) $Mg_{0.75}Al_{0.25}-Co_2Mo_{10}$ by anion exchange ($Mg_{0.75}Al_{0.25}-NO_3$ precursor); (d) $Zn_{0.67}Al_{0.33}-Co_2Mo_{10}$ by anion exchange ($Zn_{0.67}Al_{0.33}-NO_3$ precursor); (e) $Mg_{0.75}Al_{0.25}-Co_2Mo_{10}$ by LDH reconstruction ($Mg_{0.75}Al_{0.25}-$oxide precursor); (f) $Mg_{0.75}Al_{0.25}-Co_2Mo_{10}$ by anion exchange ($Mg_{0.75}Al_{0.25}-$triethyleneglycolate precursor); and (g) $Mg_{0.75}Al_{0.25}-Co_2Mo_{10}$ by anion exchange ($Mg_{0.75}Al_{0.25}-$OH precursor).

hydrolysis of the POMs in basic solutions and the partial dissolution of the LDH layers in acidic media. Hibino and Tsunashima[36] have previously reported that an ethanol/water exchange medium can appreciably reduce the degree of dissolution of the LDH layers at the autogenous pH of reaction; however, these authors did not study the effect of the reaction medium on the heptamolybdate POM hydrolysis. In this regard, the intercalation of the $[Co_2Mo_{10}]$ POM represents an interesting example for the study of this effect by observing the resulting Mo/Co molar ratios in the synthesized intercalated materials. Therefore, we present a systematic study of the $[Co_2Mo_{10}]$ anion intercalation in LDHs by anion exchange using MgAl−OH LDHs as precursors.

Five MgAl−OH LDHs with different metal ratios were utilized as precursors for the anion-exchange experiments. The experimental values of x for the LDH precursors were 0.14, 0.20, 0.26, 0.33, and 0.39. The synthesized $[Co_2Mo_{10}]$ POM presented a Mo/Co molar ratio of 5.10 as determined by ICP elemental analysis, and its powder XRD, FTIR, Raman, and TG/DTA patterns agree with the results reported in the literature for this POM.[28,37] The charge of the $[Co_2Mo_{10}]$ anion was determined by the potentiometric titration of a 0.002116 M $[NH_4]_6[H_4Co_2Mo_{10}O_{38}]$ solution (100 mL) with NaOH solution as shown in Figure 3. The equivalence point occurs at 13.9 equiv of OH^-, which corresponds to the decomposition of the anionic complex according to the following equation:

$$[H_4Co_2Mo_{10}O_{38}]^{6-} + 14OH^- \rightarrow 2Co(OH)_3 + 10MoO_4^{2-} + 6H_2O \quad (1)$$

Table 1 summarizes the different anion exchange conditions for the intercalation of the $[Co_2Mo_{10}]$ POM

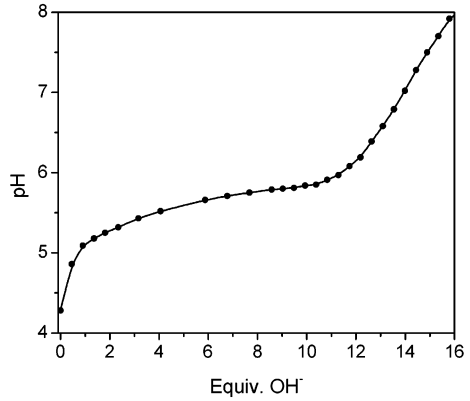

Figure 3. Potentiometric titration of 0.002116 M $[NH_4]_6[H_4Co_2Mo_{10}O_{38}]$ solution with 0.0955 M NaOH solution at 353 K.

in MgAl−OH LDHs, together with the elemental analysis of the resulting materials.

It can be clearly seen from Table 1 that the resulting intercalated materials can have different values of x and Mo/Co molar ratios depending on the precursor and the exchange conditions utilized. For example, under the same exchange reaction conditions (353 K, 0.5 h, autogenous pH, and aqueous medium) an interesting trend is observed. The larger the precursor value of x, the lower the change of x in the final product, as seen in samples S1, S2, S6, and S11 (precursor x = 0.14, 0.20, 0.26, and 0.39; % x change = 94.3, 41.6, 5.5, and −0.4, respectively). Thus, a higher content of Al^{3+} stabilizes the LDH. On the other hand, at larger precursor values of x, larger Mo/Co molar ratios in the final $[Co_2Mo_{10}]$ intercalated LDHs are observed (precursor x = 0.14, 0.20, 0.26, and 0.39; Mo/Co = 1.38, 2.34, 2.22, and 3.93, respectively). Thus, higher Al^{3+} content (and exchange capacity) stabilizes the POM intercalate. We have recently reported[38] that the dissolution of MgAl−OH LDHs in acidic media is thermodynamically favored at low values of x. This fact can explain the large dissolution observed for precursors with low values of x. Additionally, the dissolution of the MgAl−OH layers may be also related to the low Mo/Co molar ratios due to a higher hydroxyl concentration in solution, which results in the decomposition of the $[Co_2Mo_{10}]$ anion. A possible explanation of the variable Mo/Co molar ratio (<5.0) results in Table 1 may be that the solution $[Co_2Mo_{10}]$ anions are decomposed into $Co(OH)_3$, MoO_4^{2-}, and H_2O; the larger aqueous solubility of the MoO_4^{2-} in comparison with the $Co(OH)_3$ favors retention of the former in the bulk solution, giving rise to an accumulation of Co in the LDH interlayers, thus explaining the low experimental Mo/Co molar ratios.

The effect of the ethanol/water medium at autogenous pH on the metal ratios of the intercalated LDHs can be observed from the pair of samples S2(W)/S3(E) and S5(W)/S6(E) ([Mo/Co−W]/[Mo/Co−E] = 2.34/2.60 and 2.22/3.18; [% x change-W]/ [% x change-E] = 41.6/28.4 and 30.1/5.5, respectively). These results show that the presence of ethanol in the reaction medium improves the characteristics of the intercalates minimizing the change of the precursor value of x and by giving rise to

(36) Hibino, T.; Tsunashima, A. *Chem. Mater.* **1997**, *9*, 2082.
(37) Quinones, S. O.; Ivanov-Emin, B. N.; Kaziev, G. Z. *Russ. J. Inorg. Chem.* **1979**, *24*, 1826.
(38) Bravo-Suárez, J. J.; Páez-Mozo, E. A.; Oyama, S. T. *Quim. Nova*; accepted for publication.

Table 1. Meixnerite-Based Anion-Exchange Intercalations[a]

		exchange conditions						
sample	ideal formula[b]	*T*/K	*t*/h	pH	RM	experimental formula[b]	Mo/Co	% *x* change[c]
S1	$Mg_{0.86}Al_{0.14}-Co_{0.05}Mo_{0.23}$	353	0.5	A	W	$Mg_{0.73}Al_{0.27}Co_{0.30}Mo_{0.41}$	1.38	94.3
S2	$Mg_{0.80}Al_{0.20}-Co_{0.07}Mo_{0.33}$	353	0.5	A	W	$Mg_{0.72}Al_{0.28}Co_{0.25}Mo_{0.59}$	2.34	41.6
S3	$Mg_{0.80}Al_{0.20}-Co_{0.07}Mo_{0.33}$	353	0.5	A	E	$Mg_{0.75}Al_{0.25}Co_{0.21}Mo_{0.54}$	2.60	28.4
S4	$Mg_{0.74}Al_{0.26}-Co_{0.09}Mo_{0.43}$	333	0.5	A	E	$Mg_{0.73}Al_{0.27}Co_{0.14}Mo_{0.49}$	3.45	2.4
S5	$Mg_{0.74}Al_{0.26}-Co_{0.09}Mo_{0.43}$	353	0.5	A	W	$Mg_{0.66}Al_{0.34}Co_{0.25}Mo_{0.54}$	2.22	30.1
S6	$Mg_{0.74}Al_{0.26}-Co_{0.09}Mo_{0.43}$	353	0.5	A	E	$Mg_{0.73}Al_{0.27}Co_{0.16}Mo_{0.50}$	3.18	5.5
S7	$Mg_{0.74}Al_{0.26}-Co_{0.09}Mo_{0.43}$	353	0.5	4.7	W	$Mg_{0.54}Al_{0.46}Co_{0.14}Mo_{0.52}$	3.77	75.8
S8	$Mg_{0.74}Al_{0.26}-Co_{0.09}Mo_{0.43}$	353	0.5	4.7	E	$Mg_{0.56}Al_{0.44}Co_{0.14}Mo_{0.55}$	4.03	69.6
S9	$Mg_{0.74}Al_{0.26}-Co_{0.09}Mo_{0.43}$	373	16	A	W	$Mg_{0.57}Al_{0.43}Co_{0.28}Mo_{0.52}$	1.89	63.8
S10	$Mg_{0.67}Al_{0.33}-Co_{0.11}Mo_{0.56}$	353	1	4.7	E	$Mg_{0.66}Al_{0.34}Co_{0.09}Mo_{0.48}$	5.04	1.4
S11	$Mg_{0.61}Al_{0.39}-Co_{0.13}Mo_{0.65}$	353	0.5	A	W	$Mg_{0.61}Al_{0.39}Co_{0.11}Mo_{0.41}$	3.93	−0.4
S12	$Mg_{0.61}Al_{0.39}-Co_{0.13}Mo_{0.65}$	353	1	A	W	$Mg_{0.60}Al_{0.40}Co_{0.11}Mo_{0.40}$	3.61	0.8
S13	$Mg_{0.61}Al_{0.39}-Co_{0.13}Mo_{0.65}$	353	1	4.3	W	$Mg_{0.63}Al_{0.37}Co_{0.11}Mo_{0.51}$	4.53	−4.9
S14	$Mg_{0.61}Al_{0.39}-Co_{0.13}Mo_{0.65}$	353	1	4.7	W	$Mg_{0.62}Al_{0.38}Co_{0.11}Mo_{0.52}$	4.60	−3.0
S15	$Mg_{0.61}Al_{0.39}-Co_{0.13}Mo_{0.65}$	353	1	4.7	E	$Mg_{0.60}Al_{0.40}Co_{0.10}Mo_{0.48}$	5.00	2.0
S16	$Mg_{0.61}Al_{0.39}-Co_{0.13}Mo_{0.65}$	353	3	4.7	E	$Mg_{0.60}Al_{0.40}Co_{0.09}Mo_{0.48}$	5.26	0.8
S17	$Mg_{0.61}Al_{0.39}-Co_{0.13}Mo_{0.65}$	353	5	4.7	E	$Mg_{0.62}Al_{0.38}Co_{0.09}Mo_{0.50}$	5.46	−2.3

[a] *T* = temperature of reaction, *t* = time of reaction, RM = reaction medium, $x = Al^{3+}/(Mg^{2+} + Al^{3+})$, A = autogenous pH, W = water solution, E = ethanol/water solution. [b] Based on POM total exchange of a MgAl−OH precursor. $[Mg_{1-x}Al_x(OH)_2][H_4Co_2Mo_{10}O_{38}]_{x/6}$ [c] % *x* change = [(precursor *x* value − final product *x* value)/(precursor *x* value)]·100.

Mo/Co ratios close to 5.0. Similar results have been reported for the anion exchange of the heptamolybdate ($[Mo_7O_{24}]^{6-}$) intercalated MgAl LDH prepared in an ethanol/water solution at autogenous pH where a reduction in the dissolution of the LDH layers is observed.[36] When the pH of the reaction is reduced to 4.7 the benefit noticed with the ethanol/water reaction medium in preventing the dissolution of the MgAl−OH LDH layers is not significantly present, as can be seen in the pair of samples S7(W)/S8(E) and S14(W)/S15(E) [% *x* change-W]/[% *x* change-E] = 75.8/69.6 and −3.0/2.0, respectively). On the other hand, the Mo/Co ratios are higher, probably due to a direct result of the lower pH conditions ([Mo/Co−W]/[Mo/Co−E] = 3.77/4.03 and 4.60/5.00, respectively). From samples S4 and S9 (using $Mg_{0.74}Al_{0.26}$−OH precursor) it is seen that by modifying the temperature, the reaction medium, and the time of the exchange reaction, the change in the values of *x* and the Mo/Co ratios are not appreciably improved.

In the intercalation of LDH precursors with large values of *x* (*x* = 0.33 and 0.39, at 353 K and 1 h reaction conditions) an improved resistance to dissolution of the MgAl layers is observed (change of *x* values lower than 5%) regardless of the exchange conditions used. The Mo/Co ratios also showed better results, especially when the exchange was carried out at low values of pH and in ethanol/water exchange medium. From the results presented in Table 1, typical optimum conditions involve trade-offs among the different reaction variables, mainly requiring conditions such that the $[Co_2Mo_{10}]$ anion and the LDH layers are quite stable. These conditions can be achieved using MgAl−OH precursors of large values of *x* (*x* > 0.33) at 353 K, about 1 h of reaction, pH of about 4.7, and ethanol/water medium as in samples S10 and S15. From these latter samples, the Mo/Al ratio is a good indicator of the extent of the exchange of hydroxyl anions present in the meixnerite precursor for the $[Co_2Mo_{10}]$ anions. For a total exchange the theoretical Mo/Al value is given by 10/6 = 1.67. This value is, however, never reached in samples S10 (Mo/Al = 1.41) and S15 (Mo/Al = 1.20) which only show 84.4 and 71.9% exchange, respectively. We have recently proposed[30] an equation to estimate the average interpillar distance

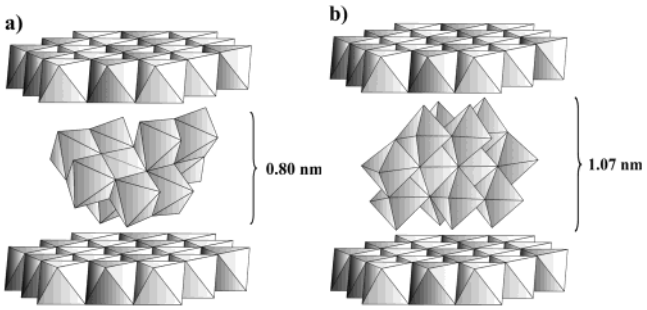

Figure 4. Two possible orientations of $[Co_2Mo_{10}]$ anion in the interlayer space of layered double hydroxides: (a) $[Co_2Mo_{10}]$ with its "main" C_2 axis parallel to the brucite-like layers; and (b) $[Co_2Mo_{10}]$ with its "secondary" C_2 axis parallel to the brucite-like layers.

(IPD) among the LDH interlayer anion pillars assuming total anion exchange:

$$\mathrm{IPD} = a\sqrt{n/x} - d_p \qquad (2)$$

Where *a* is one of the unit cell parameters of a LDH having 3R symmetry and corresponds to the mean distance between OH groups in the same side of a layer. The value of *a* can be calculated from the position of the (110) peak in the PXRD diagram ($2\theta \sim 60°$) by $a = 2d_{110}$. The parameter *n* is the charge of the anion, *x* is the molar ratio Al/(Mg+Al), and d_p is the average diameter of the top view area of the intercalated anion. In the case of the $[Co_2Mo_{10}]$ anion two possible orientations (a) and (b) in the LDH interlayers are given in Figure 4. The top view areas of these two orientations are approximately 1.052 and 0.955 nm^2, respectively.[30] The average value of parameter *a* for the $[Co_2Mo_{10}]$ intercalated LDHs is 0.305 nm.

If a circular top view area for the $[Co_2Mo_{10}]$ anion orientations is assumed, then the IPDs for the intercalated LDHs samples S10 and S15 are, for anion orientation (a), 0.126 and 0.024 nm, respectively, and for anion orientation (b), 0.180 and 0.078 nm, respectively. These values of IPDs can explain the partial anion exchanges observed in these latter samples, where, probably due

to steric restrictions, the total exchange of $[Co_2Mo_{10}]$ anions might not be feasible, because this would place the anions too close to each other. Also, because the IPD of sample S10 is larger than that for sample S15, it is expected that sample S10 will show a higher anion exchange, in agreement with the experimental results. The IPDs of partially intercalated LDHs can also be calculated by an equation similar to eq 2:

$$\mathrm{IPD} = a\sqrt{n/(\mathrm{IF}\cdot x)} - d_p$$

where IF corresponds to the intercalated fraction of the anion in the LDH. Then, the IPDs for samples S10 and S15 as calculated for anion orientation (a) are 0.240 and 0.236 nm, respectively, and for anion orientation (b) are 0.294 and 0.290 nm, respectively. For each anion orientation the values of IPDs are surprisingly similar. It should be noted that because the LDHs are not fully exchanged, they may accommodate additional interlayer charge-compensating hydroxyl anions and water molecules (diameter ~0.270 nm), especially with anion orientation (b). Attempts to increase the extent of the $[Co_2Mo_{10}]$ exchange in sample S15 by increasing the time of the exchange reaction resulted in values of Mo/Co ratio larger than 5.0 as shown in samples S16 and S17.

It is noted from reported LDHs intercalated with high-nuclearity POMs that the value of x for the LDH precursors has usually been 0.33[19,20] (coinciding with our optimum values of x for the intercalation of $[Co_2Mo_{10}]$ POM), even for LDHs containing in the layers more acidic cations such as Cu^{2+}, Ni^{2+}, Zn^{2+}, Co^{2+}, Cr^{3+}, and Ga^{3+}. LDHs with values of x of about 0.33 have been typically characterized by long-range cation ordering where the heterovalent cations have to be distributed in such a way that each M^{3+} position is surrounded by six M^{2+} positions, and each M^{2+} site has three M^{3+} and three M^{2+} sites as the nearest neighbors.[39] This arrangement of cations in the brucite-like layers seems to stabilize the LDH structure against dissolution in acidic media.

Figure 5 shows the PXRD diagrams of the parent MgAl−OH LDHs and of several $[Co_2Mo_{10}]$ intercalated samples. The PXRD diagrams for the MgAl−OH samples (Figure 5a) show well-defined peaks that agree with those expected for meixnerite compounds with 3R symmetry. From these peaks, cell parameters were calculated for each of the precursors. The d_{003} value corresponds to a distance of $c/3$ at about 0.77 nm. The unit cell parameters a and c obtained for the MgAl−OH precursors are given in Table 2. Although the synthesis of the $Mg_{0.86}Al_{0.14}-CO_3$ is attainable, the preparation of the corresponding $Mg_{0.86}Al_{0.14}-OH$ may not be completely possible because the optimum synthetic range of x for the MgAl−OH compounds ($0.23 \leq x \leq 0.43$)[40−41] is different from that observed for the MgAl−CO_3 LDHs ($0.10 \leq x \leq 0.34$).[31] That is why, for the $Mg_{0.86}Al_{0.14}-OH$ sample, an impurity peak is observed at about 0.46 nm ($2\theta \sim 19.4°$) due to the presence of $Mg(OH)_2$. When comparing the PXRD diagrams of MgAl−OH LDHs with the $[Co_2Mo_{10}]$ intercalated compounds it is noted that the peak due to the basal plane (003) of the MgAl−OH LDH at about 0.77 nm is completely removed. This indicates that anion exchange has taken place, giving as a result the PXRD patterns shown in Figure 5b. These new compounds present relevant peaks at 1.45, 0.73, 0.48, and 0.36 nm which can be ascribed to the basal planes (003), (006), (009), and (0012), respectively. The gallery height of 1.45 nm is calculated from the position of peak (003), and taking the thickness of a brucite-like layer as 0.48 nm, the resulting value is 0.97 nm. The experimental gallery height is, however, smaller than the expected 1.07 nm estimated from crystallographic data for a $[Co_2Mo_{10}]$ salt[42] and represented in the anion orientation (b) given in Figure 4. This result may be explained by the presence of slightly tilted structures where the LDH−POM hydrogen bond interactions are favored or by a partial nesting of the corners of the $[Co_2Mo_{10}]$ anion into the voids of the brucite-like layers.[43] Another interesting feature of these intercalated materials is the possibility of presenting different anion interlamellar orientations. This is observed by the presence of peaks at 0.60 and 0.40 nm in the patterns (iv) and (v) of Figure 5b, which

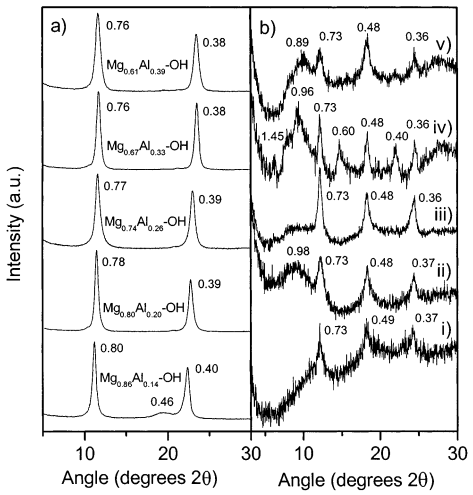

Figure 5. Powder X-ray diffraction patterns of (a) MgAl−OH precursors; and (b) $[MgAl][Co_2Mo_{10}]$ intercalated materials, where (i) Sample S1, $Mg_{0.73}Al_{0.27}Co_{0.30}Mo_{0.41}$ from $Mg_{0.86}Al_{0.14}-OH$ precursor; (ii) Sample S3, $Mg_{0.75}Al_{0.25}Co_{0.21}Mo_{0.54}$ from $Mg_{0.80}Al_{0.20}-OH$ precursor; (iii) Sample S8, $Mg_{0.56}Al_{0.44}Co_{0.14}Mo_{0.55}$ from $Mg_{0.76}Al_{0.26}-OH$ precursor; (iv) Sample S10, $Mg_{0.66}Al_{0.34}Co_{0.09}Mo_{0.48}$ from $Mg_{0.67}Al_{0.33}-OH$ precursor; and (v) Sample S15, $Mg_{0.60}Al_{0.40}Co_{0.10}Mo_{0.48}$ from $Mg_{0.61}Al_{0.39}-OH$ precursor.

Table 2. Unit Cell Parameters for MgAl−OH Precursors

	unit cell parameters, nm	
sample	a	c
$Mg_{0.86}Al_{0.14}-OH$	0.31	2.38
$Mg_{0.80}Al_{0.20}-OH$	0.31	2.36
$Mg_{0.74}Al_{0.26}-OH$	0.31	2.31
$Mg_{0.67}Al_{0.33}-OH$	0.30	2.26
$Mg_{0.61}Al_{0.39}-OH$	0.30	2.26

(39) Drits, V. A.; Bookin, A. S. In *Layered Double Hydroxides: Present and Future*; Rives, V., Ed.; Nova Science Publishers: New York, 2001; pp 39−92.
(40) Pausch, I.; Lohse, H. H.; Schürmann, K.; Allman, R. *Clays Clay Miner.* **1986**, *34*, 507.
(41) Mascolo, G.; Marino, O. *Mineral. Mag.* **1980**, *43*, 619.
(42) Nolan, A. L.; Allen, C. C.; Burns, R. C.; Craig, D. C.; Lawrance, G. A. *Aust. J. Chem.* **1998**, *51*, 825.
(43) Wang, J.; Tian, Y.; Wang, R. C.; Colón, J.; Clearfield, A. *Mater. Res. Soc. Symp. Proc.* **1991**, *233*, 63−80.

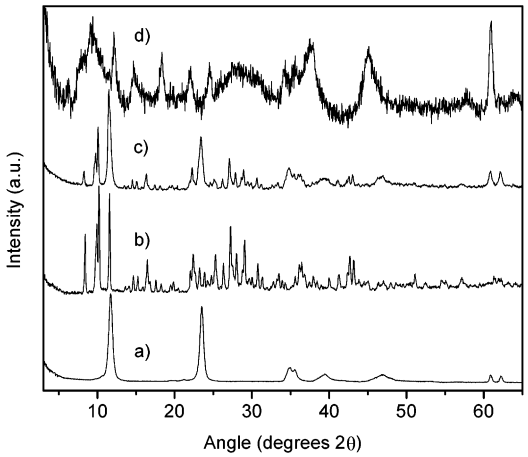

Figure 6. Powder X-ray diffraction patterns of $Mg_{0.66}Al_{0.34}$−Co_2Mo_{10} sample S10 and precursors: (a) $Mg_{0.67}Al_{0.33}$−OH; (b) $(NH_4)_6[H_4Co_2Mo_{10}O_{38}]$; (c) Physical mix at room temperature of a $Mg_{0.67}Al_{0.33}$−OH LDH with $[Co_2Mo_{10}]$ POM salt (40% of total anion exchange); and (d) Sample S10, $Mg_{0.66}Al_{0.34}Co_{0.09}$-$Mo_{0.48}$.

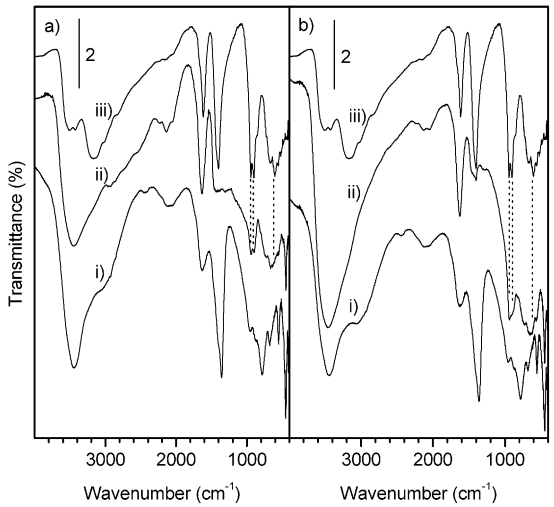

Figure 7. FTIR spectra of $[Co_2Mo_{10}]$ ammonium salt and some $[Co_2Mo_{10}]$ intercalated compounds: (a) Sample S15, $Mg_{0.60}Al_{0.40}Co_{0.10}Mo_{0.48}$; and (b) Sample S10, $Mg_{0.66}Al_{0.34}Co_{0.09}$-$Mo_{0.48}$. Spectra labeled (i) are for the MgAl−OH precursor; (ii) are for the corresponding Co_2Mo_{10} intercalated LDH; and (iii) are for the $(NH_4)_6[H_4Co_2Mo_{10}O_{38}]$ salt.

can be ascribed to basal planes (006)′ and (009)′ due to a new orientation of the $[Co_2Mo_{10}]$ intercalated anion. In these cases, the peak due to the basal plane (003)′ is masked by a broad reflection at about 0.90 nm that has been described by several authors in many LDH−POM intercalations as an impurity phase.[20,21] The position of peak (003)′ is then estimated by averaging the corresponding basal planes (006)′ and (009)′, resulting in a value of 1.20 nm. By subtracting the layer thickness (0.48 nm) from 1.20 nm the experimental gallery height is 0.74 nm, which is consistent with the height of the $[Co_2Mo_{10}]$ anion (0.80 nm) as given by orientation (a) in Figure 4. Regardless of the intercalated $[Co_2Mo_{10}]$ orientation, it seems that the peak intensity of the (003) reflection is quite weak and barely visible. The low intensity of (003) peak may be related to the high X-ray scattering power of the interlayer, out of phase with the brucite-like layer. The lack of the (003) reflection has been also reported for decavanadate ($[V_{10}O_{28}]^{6-}$) and heptamolybdate ($[Mo_7O_{24}]^{6-}$) intercalates.[25,36] This common behavior can be attributed to a similarity in the shapes and charges of the $[V_{10}O_{28}]$,$^{6-}$ $[Mo_7O_{24}]^{6-}$, and $[H_4Co_2Mo_{10}O_{38}]^{6-}$ intercalates.

Figure 6 shows a comparison among the PXRD of the $Mg_{0.67}Al_{0.33}$−OH, $[Co_2Mo_{10}]$ ammonium salt, a physical mixture of $Mg_{0.67}Al_{0.33}$−OH and the $[Co_2Mo_{10}]$ ammonium salt, and the intercalated LDH sample S10. Clearly, there is no crystalline $[Co_2Mo_{10}]$ component that contributes to the PXRD of the intercalate. Additionally, the unit cell parameter *a* related to the (110) peak position (2θ ∼60°) does not change in sample S10 in comparison with the parent $Mg_{0.67}Al_{0.33}$−OH LDH.

Additional evidence for the intercalation of the $[Co_2Mo_{10}]$ anions is provided by IR and Raman spectroscopy. The FTIR spectra in the range 4000−400 cm^{-1} of the MgAl−OH precursors (x = 0.33 and 0.39), the corresponding $[Co_2Mo_{10}]$ intercalates, and the $[Co_2Mo_{10}]$ ammonium salt are given in Figure 7. The peaks observed in the FTIR spectra of the MgAl−OH precursors coincide with those reported for these compounds,[44] and the FTIR spectrum of the $[Co_2Mo_{10}]$ ammonium salt is also in agreement with the previously reported spectrum for this salt.[28,37] The $[Co_2Mo_{10}]$ ammonium salt FTIR spectrum can be divided into different regions: (1) 3600−2800 cm^{-1}, which corresponds to the O−H and N−H stretchings; (2) 1700−1400 cm^{-1}, which corresponds to the region of the O−H and the N−H bendings; (3) 1000−850 cm^{-1}, which corresponds to the antisymmetric and symmetric stretches of the terminal O═Mo═O groups (Quinones et al.[37] have also proposed the assignment of the region 870−850 cm^{-1} to the vibrations of the groups Mo−(OH)−Mo or Mo−(OH)−Co); and (4) 750−550 cm^{-1}, which are assignable to Mo−O−Mo bridge stretchings. The bands at low wavenumbers 555−320 cm^{-1} correspond to complex vibrations involving the Co−O and Mo−O bands. The FTIR spectra of the intercalated compounds clearly show new peaks in the range 1000−850 cm^{-1} and 750−550 cm^{-1}, which corresponds to the intercalated compound. Terminal O═Mo═O stretching peaks are recorded at 932 and 894 cm^{-1} for sample S10, and 936 and 898 cm^{-1} for sample S15, while the corresponding $[Co_2Mo_{10}]$ peaks are recorded at 943 and 905 cm^{-1}. Comparing these results, it is noted that these $[Co_2Mo_{10}]$ characteristic bands are shifted about 10 cm^{-1} to lower wavenumbers in the intercalated compounds, probably due to the restricted geometry in the interlayer region and strong LDH−POM hydrogen bond interactions. Similar results were observed in the laser Raman studies. A peak shift to lower wavenumbers, in the 1000−850 cm^{-1} region, was also noted in the Raman spectra of the $[Co_2Mo_{10}]$ intercalated compounds (samples S15 and S10 in Figure 8), where, for example, the largest O═Mo═O terminal stretching band for the $[Co_2Mo_{10}]$ ammonium salt is recorded at 943 cm^{-1}, while for samples S15 and S10 it is recorded at 927 and 933 cm^{-1}, respectively. Comparison of FTIR and Raman spectra of the pure $[Co_2Mo_{10}]$ and the intercalated samples clearly shows that the intact ions are retained in the LDH layers. The fact that the intercalation reactions for samples S10 and S15

(44) Kagunya, W.; Baddour-Hadjean, R.; Kooli, F.; Jones, W. *Chem. Phys.* **1998**, *236*, 225.

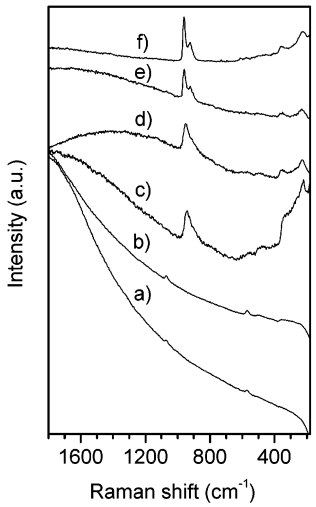

Figure 8. Raman spectra of $[Co_2Mo_{10}]$ intercalated compounds and their precursors: (a) $Mg_{0.61}Al_{0.39}$−OH; (b) $Mg_{0.67}Al_{0.33}$−OH; (c) Sample S15, $Mg_{0.60}Al_{0.40}Co_{0.10}Mo_{0.48}$; (d) Sample S10, $Mg_{0.66}Al_{0.34}Co_{0.09}Mo_{0.48}$; (e) Physical mixture at room temperature of a $Mg_{0.67}Al_{0.33}$−OH LDH with $[Co_2Mo_{10}]$ POM salt (40% of total anion exchange); and (f) $(NH_4)_6[H_4Co_2Mo_{10}O_{38}]$ salt.

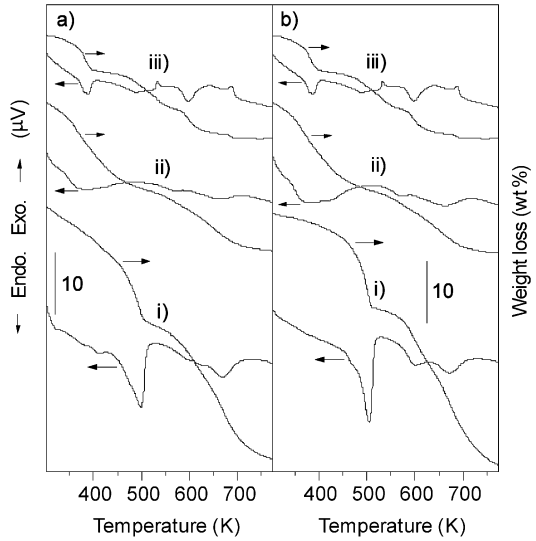

Figure 9. TGA and DTA curves for $[Co_2Mo_{10}]$ intercalated compounds and their precursors: (a) Sample S15, $Mg_{0.60}Al_{0.40}Co_{0.10}Mo_{0.48}$; and (b) Sample S10, $Mg_{0.66}Al_{0.34}Co_{0.09}Mo_{0.48}$. Spectra labeled (i) are for the MgAl−OH precursor; (ii) are for the corresponding MgAl−Co_2Mo_{10} intercalated compound; and (iii) are for the $(NH_4)_6[H_4Co_2Mo_{10}O_{38}]$ salt.

were carried out at a pH in which the $[Co_2Mo_{10}]$ POM and the MgAl−OH LDH precursor are stable, and also that MoO_4^{2-} decomposition product was not detected by Raman spectroscopy, support that highly pure $[Co_2Mo_{10}]$ POM is the intercalated specie in these LDH samples.

The thermal stabilities of the $[Co_2Mo_{10}]$ intercalated LDHs were determined by TG/DTA, XRD, IR, and rehydration experiments of samples dried at different temperatures. Figure 9 shows the TG/DTA profiles for samples S15 and S10, and their precursors. The TGA diagram for the ammonium salt $(NH_4)_6[H_4Co_2Mo_{10}O_{38}]\cdot 7H_2O$ (Figure 9a curve iii) presents several plateaus. In the first plateau, 6.5 molecules of water are lost at 433 K and 9.0 are lost at 502 K. The most relevant features in the corresponding DTA profile are the exothermic effect at 533 K that has been previously assigned to the crystallization of amorphous decomposition products.[37] These products may include the dehydrated $(NH_4)_3[CoMo_6H_6O_{24}]$ Anderson phase, $(NH_4)[CoMo_4O_{14}]$, $CoMoO_4$, MoO_3, and the intermediate molybdic phase $[(NH_4)_2O]xMoO_3]\cdot zH_2O$.[28] The weight loss from 502 to 649 K (where the DTA minimum at 598 K has been completed) represents an 8.6% change, which is in agreement with the calculated 8.0% corresponding to the loss of water and ammonia from the dehydrated $[Co_2Mo_{10}]$ salt. The weight loss up to 773 K represents 16.8% of the initial sample weight. The TG/DTA profiles of the MgAl−OH precursors (Figure 9a curve i and 9b curve i) present features similar to those of previously reported LDHs intercalated with small anions, i.e., CO_3^{2-}, NO_3^-, Cl^-, etc.[45] Main DTA minima are observed at about 503 (corresponding to the loss of extracrystalline and interlayer water), 603, and 672 K (corresponding to the dehydroxylation of the brucite-like layers and the loss of the interlayer hydroxyl anions). The observed weight loss from 298 to 773 K for the MgAl−OH precursors is about 41% of the initial sample weight and for the dehydrated precursors is about 25% which is close to the theoretical value, 32%, required for the formation of the corresponding oxides. The TG/DTA of the intercalated LDH samples S15 and S10 are shown in Figure 9a curve ii and 9b curve ii, respectively. For sample S15 (Figure 9a curve ii) three main DTA features are observed. The first one is composed of some overlapped minima that extends up to 488 K corresponding to a loss of 13.6% of the initial sample weight and which can be ascribed to the loss of extracrystalline and interlayer water. This result together with the chemical analysis in Table 1 gives the following calculated formula for sample S15:

$$[Mg_{0.60}Al_{0.40}(OH)_2][H_4Co_2Mo_{10}O_{38}]_{0.288/6}(OH)_{0.112}\cdot 1.24H_2O$$

Two other DTA features are recorded at 573 and 666 K. The observed weight loss from 488 to 724 K (where the DTA minimum at 666 K has been completed) can be ascribed to the removal of $[Co_2Mo_{10}]$ structural water and the interlayer hydroxyl groups, and the partial dehydroxylation of the brucite-like layers. The DTA minimum centered at 573 K presents a weight loss of 3.8% (from 488 to 598 K) and may be tentatively assigned to the loss of $[Co_2Mo_{10}]$ structural water and hydroxyls bonded to Al metals, which present theoretical values of 1.2 and 2.5%, respectively. The DTA minimum at 666 K presents a weight loss of 6.2% (from 598 to 724 K) and has been assigned to a partial loss of interlayer hydroxyls (1.4% theoretical) and hydroxyls bonded to Mg metals (7.6% theoretical). The total weight loss up to 773 K was 24.0%, a lower value than that for the original MgAl−OH precursor which may be because the $[Co_2Mo_{10}]$ species are not removed during the calcination process. Similar results are obtained for sample S10 (Figure 9b curve ii): overlapped DTA minima ending at about 502 K, and minima at 573 and

(45) Rives, V., Ed. *Layered Double Hydroxides: Present and Future*; Nova Science Publishers: New York, 2001; pp 115−137.

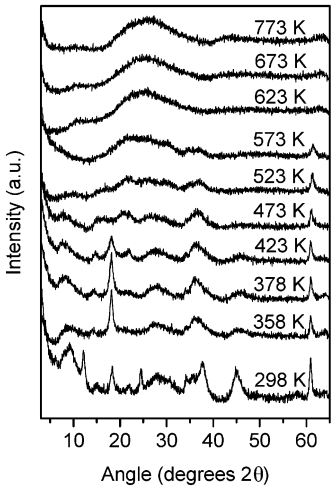

Figure 10. Powder X-ray diffraction patterns of sample S10, $Mg_{0.66}Al_{0.34}Co_{0.09}Mo_{0.48}$, dried under vacuum for 12 h at different temperatures.

663 K. A loss of 14.0% is observed up to 502 K, which gives a calculated formula for sample S10 of

$$[Mg_{0.66}Al_{0.34}(OH)_2][H_4Co_2Mo_{10}O_{38}]_{0.287/6}(OH)_{0.053}\cdot 1.28H_2O$$

Similarly to the results of sample S15, the observed weight loss for the DTA minimum at 573 K (3.4%) matches the theoretical losses corresponding to the loss of $[Co_2Mo_{10}]$ structural water (1.2%) and hydroxyls bonded to Al metals (2.2%). Also, the weight loss of 6.4% between 594 and 722 K may correspond to the partial loss of interlayer hydroxyls (0.7% theoretical) and hydroxyls bonded to Mg metals (8.5% theoretical). The total weight loss up to 773 K of sample S10 was 24.3% the initial sample weight, similar to that obtained for sample S15. In general, it seems that $[Co_2Mo_{10}]$ intercalated LDH layers can be thermally stable up to temperatures of about 573 K. The conclusion of the thermal analysis is that the intercalated material is stable up to 573 K, with decomposition of the $[Co_2Mo_{10}]$ beginning at 503 K.

The previous thermal assignments are further verified by PXRD of sample S10 outgassed at different temperatures for 12 h (Figure 10). As the temperature is increased from room temperature up to 423 K, the intercalated sample changes its PXRD pattern. Basal reflections due to orientation (b) of the intercalated $[Co_2Mo_{10}]$ anion (Figure 4) are significantly reduced in intensity and shifted to lower *d* spacings corresponding to tilted structures and finally reaching a *d* spacing value corresponding to $[Co_2Mo_{10}]$ orientation (a) (Figure 4). Additionally to this shifting, an intense reflection at 0.49 nm is observed. A similar reflection has been reported for $Mg_{0.64}Al_{0.36}-Mo_7O_{24}$ intercalated compounds heated to 423 K and has been assigned to a change in the arrangement of anions in the interlayers.[36] The PXRD of sample S10 heated at 473 K shows that the ordered lamellar structure is lost, presenting broad and weak maxima around 1.14, 0.58, 0.44, 0.33, and 0.25 nm. This disordered structure is a direct result of the elimination of the interlayer water as shown in its TG/DTA profile (Figure 9b curve ii). For the sample heated at 523 K, similar features are observed but they

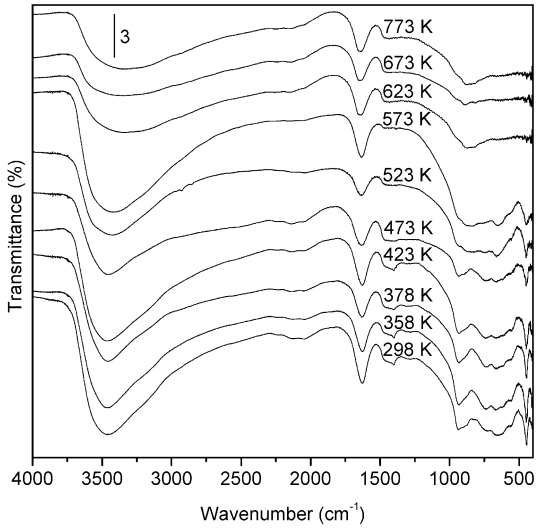

Figure 11. FTIR spectra of sample S10, $Mg_{0.66}Al_{0.34}Co_{0.09}Mo_{0.48}$, dried under vacuum for 12 h at different temperatures.

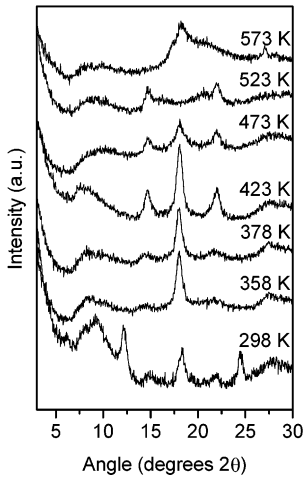

Figure 12. Powder X-ray diffraction patterns of rehydrated sample S10, $Mg_{0.66}Al_{0.34}Co_{0.09}Mo_{0.48}$, at room temperature for 3 days after being dried under vacuum for 12 h at different temperatures.

are of lower intensity. Over 523 K and up to 773 K, a big and very broad peak around 0.35 nm is recorded. This feature could be related to the formation of amorphous oxidic species. It is also noted that the (110) peak close to 0.15 nm remains in the same position up to 573 K indicating that these materials are still lamellar and related to the original sample. This result is in agreement with the DTA minimum at 573 K representing the partial loss of layered hydroxyls.

Figure 11 presents the FTIR spectra of sample S10 outgassed at different temperatures. As seen in this figure, the characteristic Mo−O and Mo−O−Mo stretching frequencies (1000−850 and 750−550 cm^{-1}, respectively) are retained up to 573 K, the temperature at which the DTA minimum for the dehydroxylation of the $[Co_2Mo_{10}]$ is found. However, samples at 523 and 573 K present band broadening to lower frequencies at 894 cm^{-1}. This may point out that the $[Co_2Mo_{10}]$ anion has been partially degraded and new [CoMo] species are formed. Over 573 K and up to 773 K several observations can be made: (a) the flattening of fine absorption of the IR spectrum also indicates the decomposition of the intercalated $[Co_2Mo_{10}]$ anions; and (b) the reduction

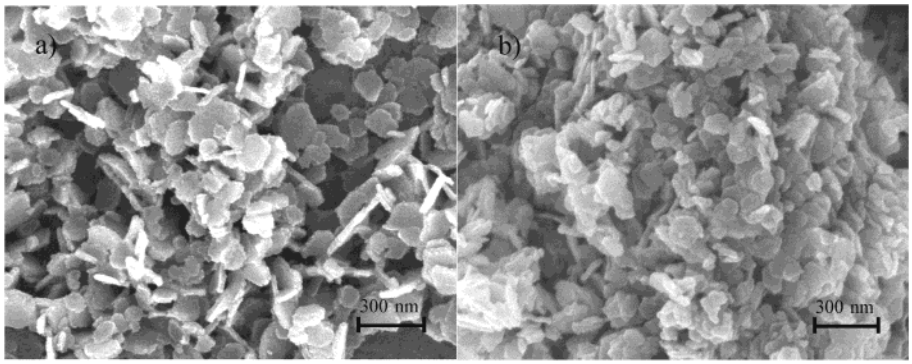

Figure 13. SEM images of sample S10, $Mg_{0.66}Al_{0.34}Co_{0.09}Mo_{0.48}$, (a) dried at room temperature; and (b) dried under vacuum at 773 K for 12 h.

in intensity of the layers M−OH stretching modes present in the broad band around 3400−3500 cm^{-1} also agrees with the partial dehydroxylation of the LDH layers as shown in the TG/DTA results for sample S10.[46] Additional evidence of the $[Co_2Mo_{10}]$ decomposition is given by the change in color of the intercalated samples from green at 523 K to gray at 573 K.

The thermal stability of sample S10 outgassed at different temperatures has been also studied by rehydration of the dried samples in deionized distilled water for 3 days at room temperature. The PXRD patterns of rehydrated sample S10, previously outgassed at temperatures up to 573 K, are shown in Figure 12. A comparison between the PXRD patterns in Figures 10 and 12 shows that even the dehydrated samples at 473 and 523 K whose PXRD patterns correspond to disordered structures can be rehydrated to give basal reflections at 0.60 and 0.40 nm corresponding to orientation (a) of the intercalated $[Co_2Mo_{10}]$ anion (Figure 4). These results may be because these temperatures are below the temperature range 529−598 K observed for the decomposition of the $[Co_2Mo_{10}]$ ammonium salt and sample S10. The PXRD results in Figure 12 together with the FTIR spectra in Figure 11 could also indicate that in the temperature range 529−598 K the decomposition of the $[Co_2Mo_{10}]$ intercalated compound led to [CoMo] intercalates with vibrational properties similar to the decamolybdodicobaltate anion ($[CoMo_6H_6O_{24}]$, $[CoMo_4O_{14}]$, $CoMoO_4$, ...),[28] as well as metal (Mg, Al) complexes of these latter compounds.

The SEM images of sample S10 as prepared and outgassed at 773 K are shown in Figure 13. The sample dried at room temperature displays well-dispersed hexagonal platelets that resemble the morphology of the $Mg_{0.67}Al_{0.33}$−OH precursor. As seen in Figure 13a, these platelets present average thickness and diameter of about 30 and 140 nm, respectively. For this intercalated material, the initial morphology is partially retained up to 773 K (Figure 13b), at which point some intermediate amorphous metallic oxides are formed, tending to group in irregular aggregates.

TEM micrographs of sample S10 dried at room temperature also reveal the layered structure of this material. The observed well-formed hexagonal platelets present an average thickness and diameter of 27 and 140 nm, respectively, in agreement with the SEM observations.

The N_2 adsorption/desorption curves of sample S15 and sample S10 as prepared and outgassed at 773 K are presented in Figure 14. These three isotherms are similar and correspond to type IV in the IUPAC classification, which is typical of monolayer-multilayer adsorption on mesoporous solids; and an H1-type hysteresis which is often associated with interparticle mesoporosity.[47]

Table 3 shows the microporous areas and volumes of relevant samples from Table 1, including sample S10 outgassed at different temperatures together with its precursor materials. For all the $[Co_2Mo_{10}]$ intercalated samples, with the exception of sample S5, the microporous areas and volumes are small and indicate the lack of intragallery microporosity in these materials. The observed microporous properties are probably a contribution of the porosity formed from the aggregation of the platelike particles. Sample S5 presents a relatively high BET area and an appreciable microporous area and volume originating from the interlayer space. An analysis of the IPD for this material can help to explain this result. Assuming a $[Co_2Mo_{10}]$ anion orientation (a) in the LDH, a circular top view of the anion, and also that all the present molybdenum is part of the intercalated $[Co_2Mo_{10}]$ anion, then the IPDs can be calculated. It should not be forgotten that for this sample other species such as $Co(OH)_3$ may be present as a result of the excess of observed cobalt. Furthermore, the actual IPD should be calculated with values of x between that of the original precursor and the intercalated material (0.25 and 0.34, respectively) because partial dissolution of the LDH layers has occurred. The estimated IPDs are therefore 0.34 and 0.13 nm, respectively. The lack of microporosity in the rest of the samples is explained by small IPDs which restrict the access of N_2 molecules (diameter ∼0.37 nm) into the interlayers. The pillars are stacked too close to each other to give micropores. In the case of samples S10 and S15, the specific surface areas are quite similar; and for sample S10, a reduction in the BET area is observed when compared with that of the LDH precursors. We have recently reported[30] that these differences can be explained by a variation in the crystallite size and the

(46) Kloprogge, J. T.; Frost, R. L. In *Layered Double Hydroxides: Present and Future*; Rives, V., Ed.; Nova Science Publishers: New York, 2001; pp 139−192.

(47) Sing, K. S. W.; Everett, D. H.; Haul, R. A. W.; Moscou, L.; Pierotti, R. A.; Rouquérol, J.; Siemieniewska, T. *Pure Appl. Chem.* **1985**, 57, 603.

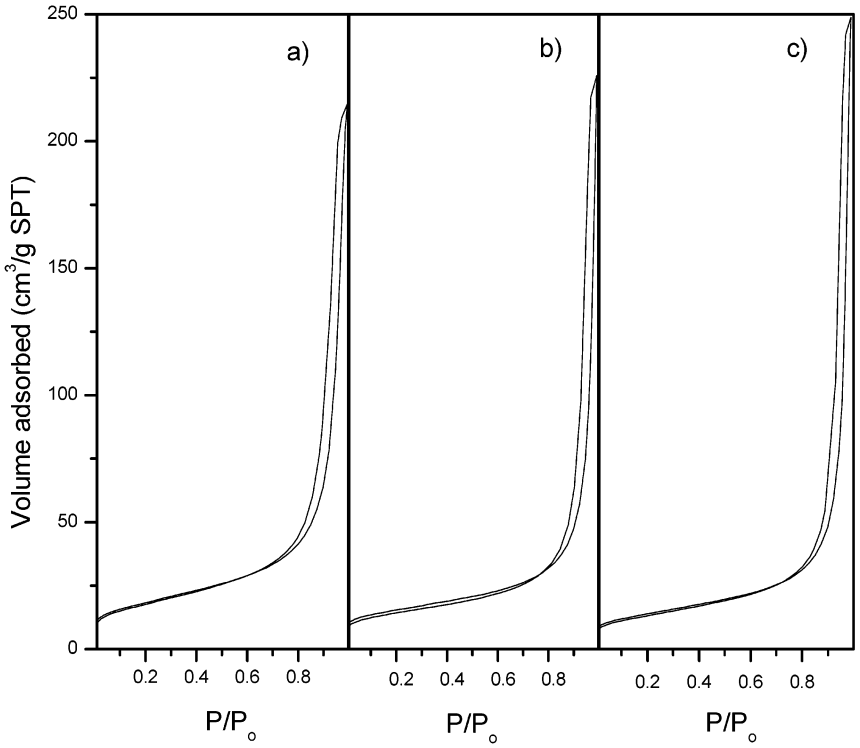

Figure 14. N_2 adsorption−desorption isotherms for (a) Sample S15, $Mg_{0.60}Al_{0.40}Co_{0.10}Mo_{0.48}$, outgassed at 378 K; (b) Sample S10, $Mg_{0.66}Al_{0.34}Co_{0.09}Mo_{0.48}$, outgassed at 378 K; and (c) Sample S10, $Mg_{0.66}Al_{0.34}Co_{0.09}Mo_{0.48}$, dried under vacuum at 773 K for 12 h.

Table 3. BET/N_2 Surface Areas (S_{BET}) and Microporous Properties (S_{micro}, V_{micro}) of [Co_2Mo_{10}] Intercalated Compounds

sample	S_{BET}, m^2/g	S_{micro}, m^2/g	V_{micro}, cm^3/g
$(NH_4)_6[H_4Co_2Mo_{10}O_{38}]$, 378 K outgassing	<1.0		
$Mg_{0.75}Al_{0.25}Co_{0.21}Mo_{0.54}$ (S3), 378 K outgassing	44.1	3.5	0.001
$Mg_{0.66}Al_{0.34}Co_{0.25}Mo_{0.54}$ (S5), 378 K outgassing	141.0	31.8	0.026
$Mg_{0.65}Al_{0.35}-CO_3$ (S10 precursor), 378 K outgassing	81.4	4.2	0.002
$Mg_{0.67}Al_{0.33}-OH$ (S10 precursor), 378 K outgassing	71.9	4.6	0.002
$Mg_{0.66}Al_{0.34}Co_{0.09}Mo_{0.48}$ (S10), 378 K outgassing	53.5	13.9	0.007
$Mg_{0.66}Al_{0.34}Co_{0.09}Mo_{0.48}$ (S10), 473 K outgassing	50.8	8.8	0.004
$Mg_{0.66}Al_{0.34}Co_{0.09}Mo_{0.48}$ (S10), 573 K outgassing	56.3	1.8	0.000
$Mg_{0.66}Al_{0.34}Co_{0.09}Mo_{0.48}$ (S10), 673 K outgassing	50.7	6.2	0.003
$Mg_{0.66}Al_{0.34}Co_{0.09}Mo_{0.48}$ (S10), 773 K outgassing	49.3	4.4	0.002
$Mg_{0.60}Al_{0.40}Co_{0.10}Mo_{0.48}$ (S15), 378 K outgassing	64.8	5.8	0.002

metal−anion composition of each intercalated material. For example, typical $MgAl-CO_3$ LDHs can have a crystallite thickness and a diameter of 15 and 150 nm, respectively, giving rise to external surface areas of about 80 m^2/g, similar to the experimental BET areas of sample S10 precursors. When these LDHs are intercalated with heavy POM anions, the external surface areas expressed per unit weight are lower as a direct result of a larger crystallite molecular weight. The average thickness and diameter of the LDH crystallite for sample S10 dried at room temperature as determined by SEM and TEM microscopies are 28.5 and 140 nm, respectively. Using a procedure described previously,[30] the estimated specific external surface area for this sample is 45 m^2/g, which agrees with the experimental value of 40 m^2/g. When sample S10 is outgassed at increasing temperatures up to 773 K, no noticeable changes in the specific surface areas are observed. These results are in agreement with SEM observations of sample S10 outgassed at 773 K which pointed out that this material still retains the morphology of the starting compound, and also explains the similarity of its N_2 adsorption/desorption curve with those of the unheated intercalated materials.

Conclusions

In the present study novel layered double hydroxides (LDHs) phases intercalated by the decamolybdodicobaltate(III) polyoxometalate (POM) were obtained by anion-exchange methods. Theoretical predictions of the textural properties of these intercalated compounds have indicated that microporous materials could be obtained if intercalation was carried out with LDHs presenting values of x lower than 0.25. We found that under the reaction conditions of this work this intercalation is not possible due to the dissolution of the magnesium from the LDH layers and partial hydrolysis of the [Co_2Mo_{10}] POM. Pure and crystalline intercalated compounds were only obtained at a pH of 4.7 and values of x of the LDHs larger than 0.33 (where the POM and the LDH are stable). At such relatively high aluminum substitution theoretical textural calculations predict low microporosity because of close packing of the pillars. This is confirmed by pore size distribution and surface area determinations. The PXRD results revealed that the intercalated [Co_2Mo_{10}] anions presented two different types of orientations whose gallery heights were 0.74 and 0.97 nm, respectively, the lower of which was more

stable. Thermal stability measurements of these materials by different techniques (TG/DTA, FTIR, and PXRD) showed that the $[Co_2Mo_{10}]$ was stable in the interlayers up to 523 K and the layer structure collapsed at 573 K, forming amorphous phases, although maintaining their external morphology up to 773 K.

Acknowledgment. We acknowledge financial support for this work by the Director, Division of Chemical and Thermal Systems of the National Science Foundation under grant CTS-0321979, and from Universidad Industrial de Santander and COLCIENCIAS (Colombian Institute for the Development of Science and Technology) under project 1102-05665-95. The FE-SEM work was made possible by the National Science Foundation under grant 9975678. We also thank Dr. G. L. Wilkes for use of the TG/DTA thermal analyzer and J. Sheth for making the TG/DTA measurements.

CM034853C